

DES Turbulence Modeling on the C-130 Comparison between Computational and Experimental Results

Malcolm P. Claus,[‡] Scott A. Morton,* and Russell M. Cummings,[†]
United States Air Force Academy, Department of Aeronautics
2410 Faculty Drive, Suite 108
USAF Academy, CO 80840-6400, USA.

Yannick Bury^Δ
Department of Mechanics and Fluids, ENSICA
Toulouse, FRANCE

ABSTRACT

This paper represents the results from the initial phase of a research program to determine the flow characteristics of the C-130 Hercules transport aircraft. The initial phase of the program consists of evaluation and comparison of the flow-field obtained from flow visualization methods. Specifically CFD (Computational Fluid Dynamics) results are compared with experimental Hot Wire results produced by wind tunnel tests on the C-130 in clean configuration. This paper outlines the results to date and provides a description of further work. The CFD element of this research features the use of Detached Eddy Simulation (DES) in order to extend its use as a reliable method for use on complex flow-fields. DES combines the efficiency of a Reynolds-averaged turbulence model near the wall with the fidelity of LES (Large Eddy Simulation) in separated regions. Because of the LES treatment in separated regions, it provides more accurate descriptions of the geometry-dependant, three-dimensional unsteady motions resulting in regions of massive separation. The computational aspect of the research is performed at the US Air Force Academy, with subsequent wind tunnel tests (Hot Wire) being undertaken in France at ENSICA.

I. INTRODUCTION

This paper forms part of a multi-national project to determine the flow-field characteristics of the C130 Hercules aircraft. Comparison with wind tunnel experiments is provided as a means to evaluate the use of DES for complex flow-fields. The investigation is split into three phases namely – comparison with wind tunnel data (in particular flow visualization results from Hot Wire technique (phase 1)), secondly - flow visualization comparison with wind tunnel results (phase 2, with a larger simplified model) and comparison with flight test data (phase 3). This paper presents work from phase 1 and outlines work for phase 2. The aim of this three phase investigation is to quantify the flow-field behavior and aerodynamic characteristics of the C-130 Hercules in both tail-gate down and door closed configurations. The majority of the work presented in this paper focuses on the clean configuration and assesses the ability of CFD to provide insight into the complex flow-field.

The use of rapid reaction forces, in particular the deployment of airborne troops or the delivery of cargo/supplies to frontline troops or humanitarian supplies for drought or other disaster relief has been a role carried out with diligence by the C-130 Hercules. The delivery of cargo or troops is by the use of the cargo bay ramp; this has a region of complex flow consisting of both a separation and subsequent recirculation zone. Problems can arise when objects are caught within this region; in particular operations are concerned with the possibility of objects nearly touching the empennage on exit from the rear door.

* Associate Professor of Aeronautics, AIAA Associate Fellow.

† Distinguished Visiting Professor, AIAA Associate Fellow.

Δ Associate Professor of Aeronautics, AIAA Member

‡ Research Engineer, AIAA Member.

Several investigators have studied the flow behind the C-130H; in a study undertaken by Johnson¹ et al. into the flow behind the C-130 they applied both experimental and computational methods to study the flow. Their study indicated some general trends – vortices, about the span-wise and longitudinal axis, tend to form in a number of different areas beneath the tail and a consistent upward flow throughout the entire region aft of the cargo bay.

In a study carried out by Galloway and McClurg² they undertook a comprehensive evaluation of the C-130H firefighting nozzle performance. They investigated solutions to a similar problem in which fire fighting chemicals caught in the aft circulation region contacted and damaged the underside of the aircraft. They concluded that extending the nozzle by 2.4 feet from the present location provided the optimal length to effectively deploy the material.

II. DETACHED-EDDY SIMULATION

DES was proposed by Spalart et al.³ The motivation for this approach was to combine Large-Eddy Simulation (LES) with the best features of Reynolds-averaged Navier-Stokes (RANS) methods. RANS methods have demonstrated an ability to predict attached flows very well with a relatively low computational cost. LES methods have demonstrated an ability to compute separated flow-fields accurately, but at a tremendous cost for configurations with boundary layers. Spalart’s DES method is a hybrid of LES and RANS, which combines the strengths of both methods.

The DES model was originally based on the Spalart-Allmaras one equation RANS turbulence model (Ref. 3). The wall destruction term is proportional to $(\tilde{\nu} / d)^2$, where d is the distance to the wall and $\tilde{\nu}$ which is related to the turbulent viscosity. When this term is balanced with the production term, the eddy viscosity becomes proportional to $\hat{S}d^2$ where \hat{S} is the local strain rate. The Smagorinski LES model varies its sub-grid scale (SGS) turbulent viscosity with the local strain rate, and the grid spacing: $\nu_{SGS} \propto \hat{S}\Delta^2$, where $\Delta = \max(\Delta x, \Delta y, \Delta z)$. If d is replaced with Δ in the wall destruction term, the S-A model will act as a Smagorinski LES model.

To exhibit both RANS and LES behavior, d in the SA model is replaced by

$$\tilde{d} = \min(d, C_{DES}\Delta).$$

When $d \ll \Delta$, the model acts in a RANS mode and when $d \gg \Delta$ the model acts in a Smagorinski LES mode. Therefore the model switches into LES mode when the grid is locally refined.

DES was implemented in an unstructured grid method by Forsythe et al.⁴ They determined the C_{DES} constant should be 0.65, consistent with the structured grid implementation of Spalart et al.³ when the grid spacing Δ was taken to be the longest distance between the cell center and all of the neighboring cell centers. A Newton sub-iteration method is used in the solution of the system of equations to improve time accuracy of the point-implicit method and approximate Jacobians. In the calculations presented below, a typical number of three Newton sub-iterations are used for all time-accurate cases.

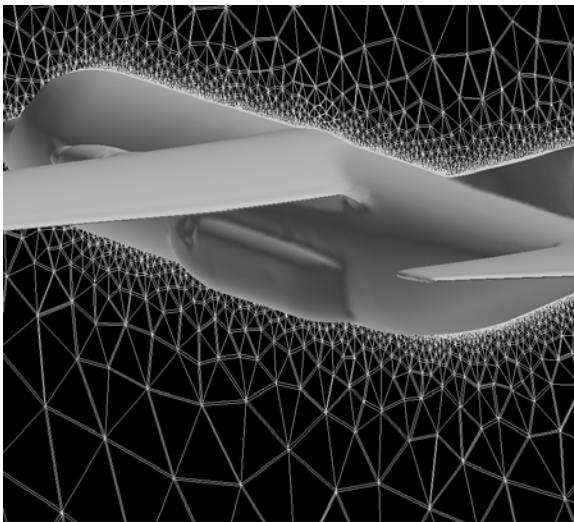
DES has successfully been applied to iced airfoils, in particular in the research undertaken by Pan and Loth⁵ on the subject showed that DES predicted the maximum lift coefficient and stall qualitatively consistent with experiments. Morton et al.⁶ applied the YPG guidelines to three massively separated flows of interest: fore-body in a cross-flow, flow over a delta wing at 27° angle of attack, and the flow over an F-15E at 65° angle of attack. The unstructured finite-volume solver *Cobalt* has been used in conjunction with DES successfully on a number of complex problems, including a supersonic base flow⁴, delta wing vortex breakdown⁷, a square with rounded corners⁸, the F/A-18C with tail buffet⁹, and the F/A-18E with unsteady shock buffet¹⁰.

III. GRID GENERATION

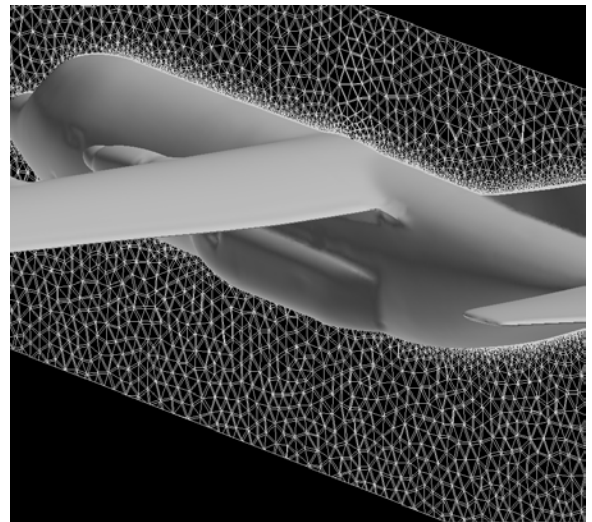
Spalart¹¹ described the process of grid design and assessment for DES, defining important regions of the solution and offering guidelines for grid densities within each region. The “Young-Person’s Guide”¹¹ (YPG) forms a basis for interpretation of many of the results presented below. One of the traditional motivations for using unstructured grids has been the ability to rapidly create grids around complex geometries. There are other positive attributes of

unstructured grids that are relevant to DES. Most notably, it is possible to concentrate points in the region of interest (i.e. in a vortex core or separated flow over a wing) and rapidly coarsen the grid away from these areas. This region of interest was termed the “focus region” in the YPG. The YPG reference describes the desirability of having isotropic grid cells in the focus region in which unsteady, time-dependent, features are resolved. For this reason, unstructured grids are good candidates for use in DES because near isotropy of the grid cells in the LES region is assured by most grid generation packages.

Comparison with wind tunnel experiments is provided as a means to evaluate the use of DES for complex flow-fields. All computational runs are performed using the CFD solver Cobalt. A half simplified aircraft model was created using Gridgen¹² with the completed grid consisting of up to 4×10^6 cells. A grid sensitivity study was undertaken, and it was determined that the original grid lacked sufficient grid points. Additional cells were incorporated into a new volume grid (Figure 1) created around the model geometry; the new volume grid extends downstream of the model and covers the planes of interest, these being the planes the hotwire measurements were obtained. Both grids have a y^+ less than one, but the new grid has an increased resolution in the region surrounding the body (Figure 1). The new grid has 6.2×10^6 cells.



(a) Original grid (4×10^6 cells)



(b) Second grid (6.2×10^6 cells)

Figure 1: Gridgen C-130 Unstructured Grid

Figure 1 shows the two grids generated for this investigation. The new grid shown in Figure 1b differs from the original grid in the number of cells; these additional cells were used in the creation of a zone of interest box, which encloses the C130. The zone of interest is shown in Figure 1b. Although an improvement over the original grid (Figure 1a), it would be advantageous for the second grid to have still more cells in the zone of interest; however, due to certain limitations this was not possible. It should be noted that additional grid sensitivity studies involving the above configuration and grid is to be carried out in the near future.

IV. ENSICA EXPERIMENTAL PROCEDURE/SET UP

The wind tunnel hot wire measurements were conducted in the low speed tunnel located in ENSICA. The model used for this study was approximately a $1/48^{\text{th}}$ scale model, producing a Reynolds number of 208,000 (based on diameter) at sea level ISA. The test Mach number was 0.12 which corresponds to a velocity of approximately 40 m/s. All measurements were taken at 0° angle of attack. Hot wire was used to determine the flow-field characteristics at various “x stations” along the centerline of the model. The datum point for these cross-sectional planes is the rear of the model (shown in Figure 3). Planes were taken upstream and down stream of this point. Figure 2 shows the model in the ENSICA wind tunnel also shown is the hotwire used to obtain velocity measurements at these points.

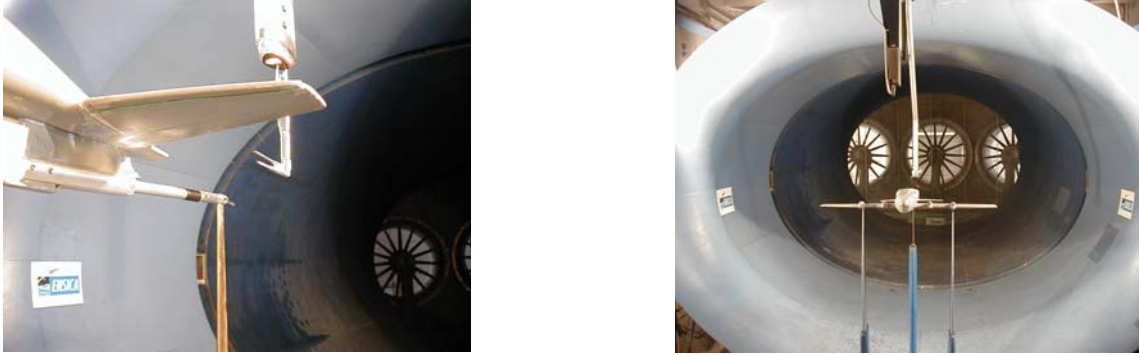


Figure 2: C-130 Model and Hotwire location in the ENSICA Wind Tunnel (courtesy of ENSICA)

A total of four positions were used in this study, along the x-axis or centerline of the model. The planes are listed in Table 1. The planes selected for investigation were chosen so as not to damage the hot wire equipment.

Station No.	Plane (X)	Plane (X, mm)
1	-0.123L	-72
2	0.057L	33
3	0.069L	40
4	0.103L	60

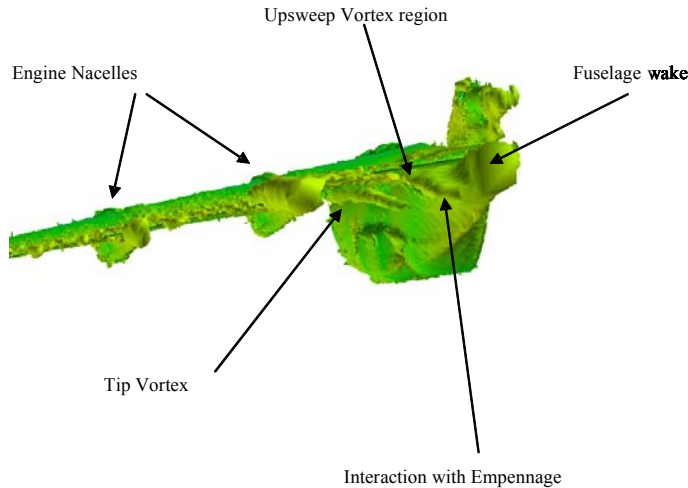
Table 1, Hot Wire cutting planes and relative position



Figure 3: C-130 Model Datum point (courtesy of ENSICA)

V. RESULTS AND DISCUSSION

Figure 4: Main Flow Characteristics



The main aim of this research is to quantify and evaluate the flow-field generated by the C130 Hercules; this is to be achieved by evaluating the results obtained from a wind tunnel test program and also CFD simulations. Before the comparison between the hot wire results and those produced by the CFD can begin it is necessary to outline some of the flow characteristics present in the complex flow field. Figure 4 illustrates some of these characteristics which dominate much of the local flow field, in particular the strong wake generated by the aft fuselage and the upsweep vortex which is produced by the interaction of the fuselage wake and the empennage. The combination of these two features occurs at about 40 mm span (measured from the

centerline of the model). At each “x-location”, a plane is generated of the vorticity produced by the model; the results indicate that the fuselage wake dominates much of the flow-field at each location of interest. In order to compare the hot wire results a CFD grid was run at the same conditions, by insuring a Reynolds number match of 208,000 (based on diameter) at a Mach number of 0.12 and using standard sea level conditions.

In order to aid the discussion of the results, additional planes have been included namely span-wise. This allows for a complete evaluation of the flow-field at this point. It should be noted that the co-ordinate system from the CFD model defers from that of the wind tunnel model/experiments, the difference is outlined in Table 2.

Co-ordinate	Wind Tunnel/ Experimental	CFD
X	Chord / length	Chord / length
Y	Span-wise	Vertical Height
Z	Vertical Height	Span-wise

Table 2, Co-ordinate System

The results from the hot wire investigation are presented as a function of normalized velocity. The plots are presented as (Velocity measured by the Hot Wire) normalized by the free-stream velocity or V_0 . The CFD results are presented as plots of vorticity in the x-direction.

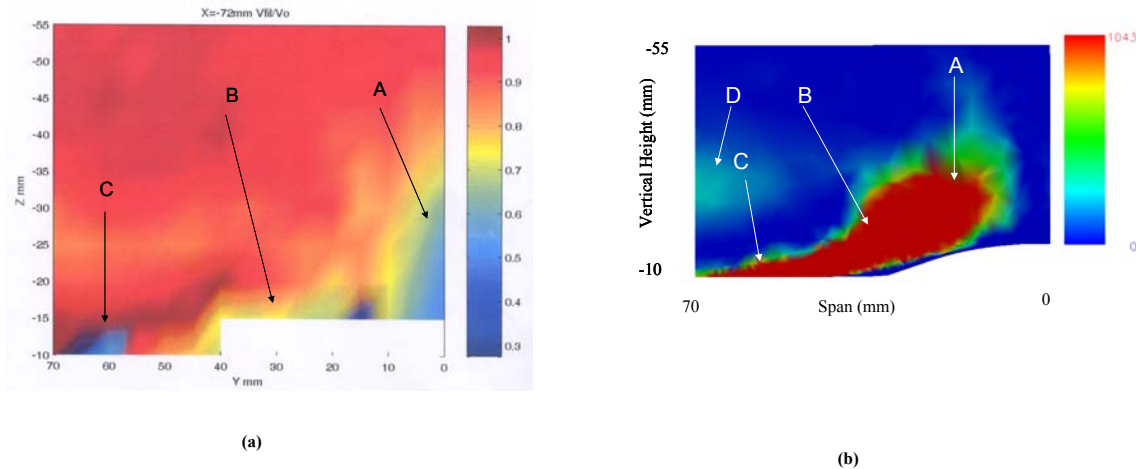


Figure 5: ENSICA and CFD results for $x = -72$ mm

Figure 5 is a comparison between the ENSICA hot wire results (Figure 5a) and the computational results (Figure 5b). Both plots show a slice through the “x- direction” approximately 72mm behind the origin position, as shown in Figure 3. The ENSICA results show normalized velocity ratio, while the CFD results show vorticity.

The grey block section shown in the lower right hand side of the plot (Figure 5a) represents the rear empennage, of the wind tunnel model; while the empennage is represented by the cut –out section illustrated in Figure 5b. The main flow characteristics for each “x-direction” slice has been identified and labeled, for discussion and comparison.

With respect to Figure 5a, a strong wake is present this is generated from the rear fuselage (denoted by A), also within the flow-field there is vortex produced at the fuselage empennage junction, at approximately 20mm span (denoted by B). The upsweep vortex travels along the underside of the empennage, until a point at approximately 60mm span where it interacts with the vortex generated by the empennage (denoted by C). The flow-field is complex within this region.

With respect to Figure 5b, the flow characteristics are denoted in the same manner as Figure 5a.

Figure 5b shows fuselage wake generated from the base of the model at the intersection of the rear door and fuselage, at this position along the x-axis the vortices begin to roll along the underside of the empennage (point A). The wake continues down the length of the ramp, the fuselage wake is strongly pronounced at a span position of 20mm from the centerline (point B). At this point an upsweep vortex is generated from the empennage. This vortex continues along the rear empennage, when at $z = 40$ mm the interaction flow generated is dominated by the vortex generated by the leading edge of the empennage (point C). The upsweep vortex decreases in strength at $z = 70$ mm (left hand side of Figure 6b). The CFD results also indicate that a small interaction region is present outside the main vortex flow-field. This interaction/vortex region (point D) is produced by the trailing edge vortex generated by the main wing.

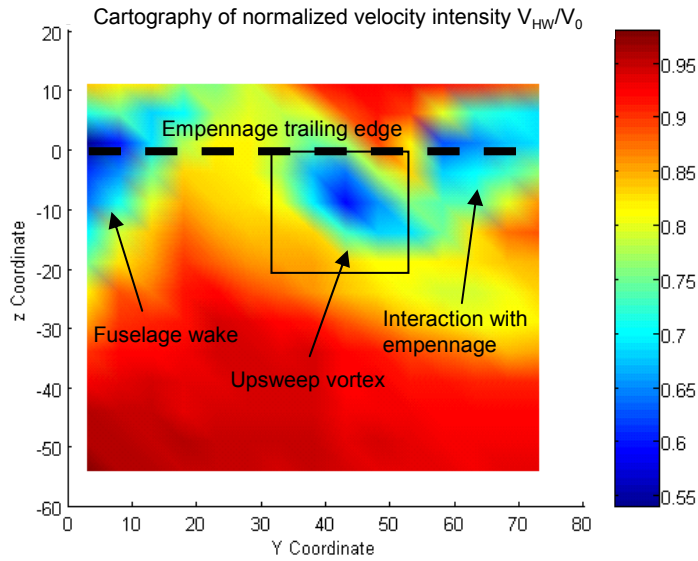
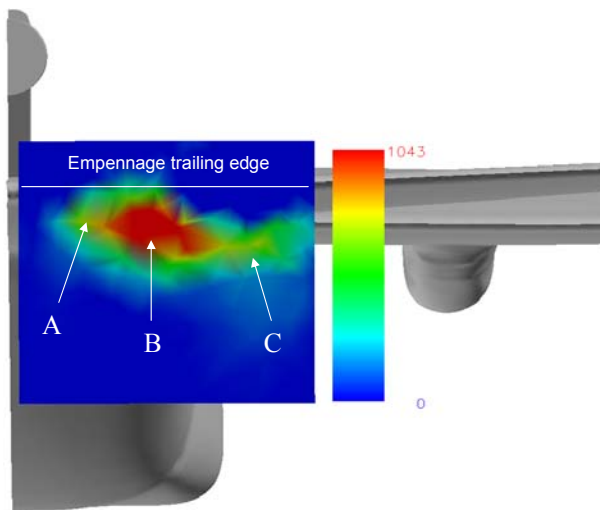


Figure 6a shows the results obtained from another “x-location” at a location 33mm ahead of the origin. The fuselage wake vortex and the upsweep vortex are still present. The trailing edge of the empennage has been included for reference.

Figure 6b depicts the corresponding CFD simulation. Again the letters correspond to the areas of interest within the flow-field. The position of the upsweep vortex can be determined from the CFD solution.



However, the CFD results do not show the interaction between the empennage and the upsweep vortex to the same degree. The hot wire results indicate that the flow in this region should be present above the empennage trailing edge especially the interaction vortex (point C, in Figure 6b). This could be due to the lack of grid refinement/ resolution available for the current grid.

Figure 6a and b, ENSICA and CFD results respectively for $x = +33$ mm

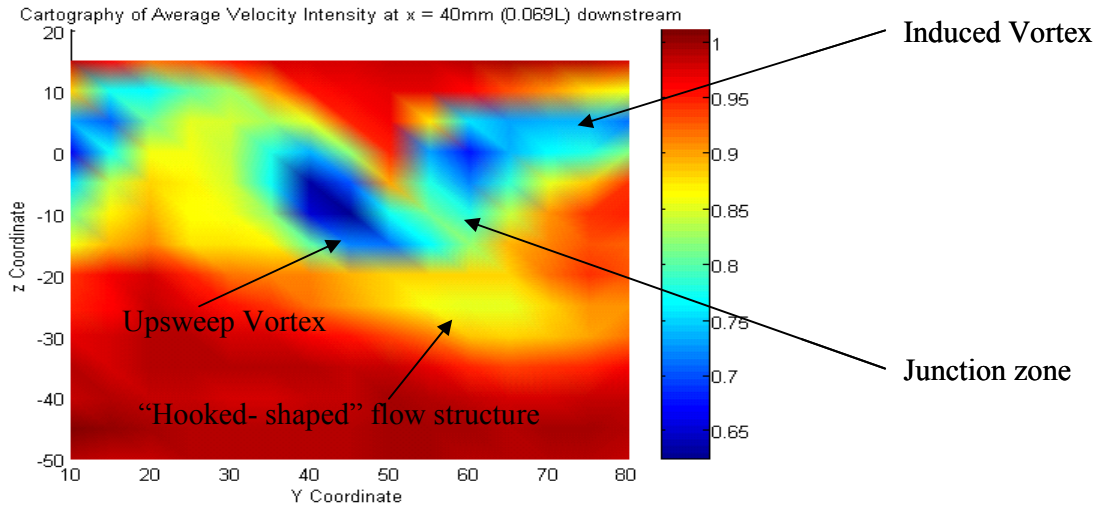


Figure 7a

Figure 7, shows the results for a position 40mm downstream of the datum point. The upsweep vortex is identified in the CFD case as well as the “Hooked Shaped flow”. In Figure 7a, there is an induced vortex present; this can clearly be seen as well as the vortex induced by the empennage. The ENSICA hot wire results also indicate the presence of a “hooked shaped” flow structure; however, it is not shown in the CFD results apart from an extremely faint region. There also does not seem to be a junction zone in the CFD results. The junction zone is located between the upsweep vortex and the induced vortex. However, this feature is not clearly visible in the CFD results. This is most probably due to the lack of grid refinement/resolution.

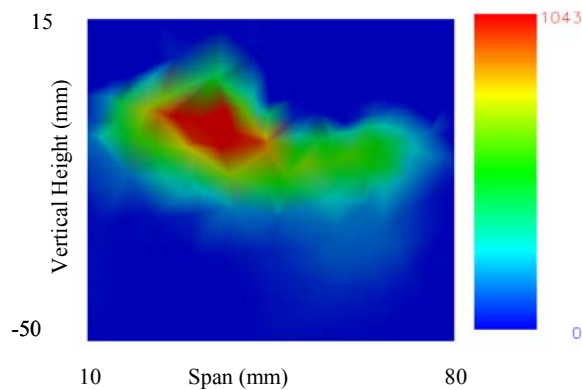


Figure 7b

**Figure 7a and b: ENSICA and CFD results respectively
(For $x = +40$ mm)**

Figure 8a

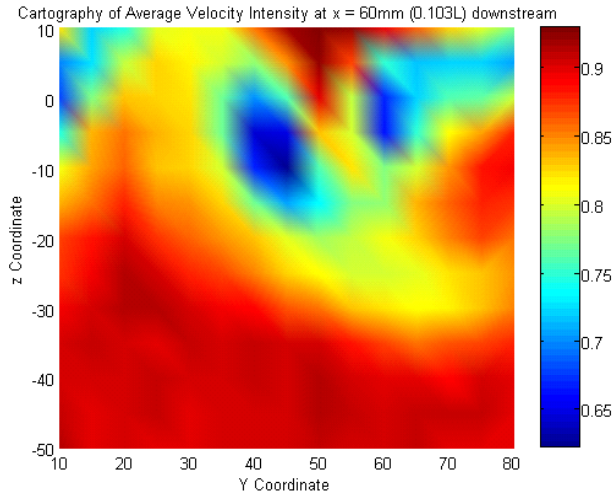
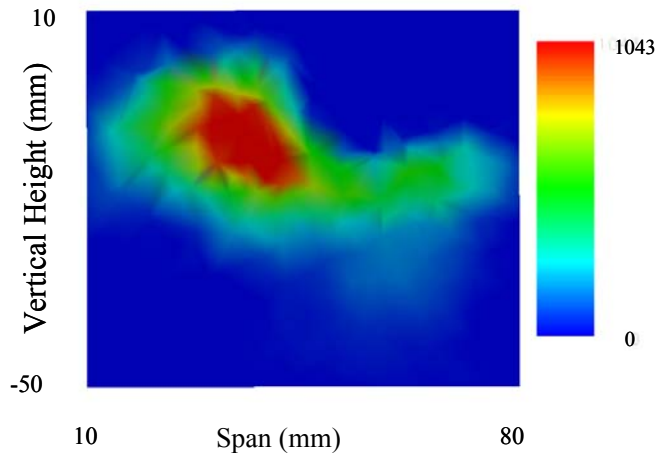


Figure 8 represents the flow field results obtained for an x location 60mm from the datum point. Again the flow field is dominated by a large vortex, namely the upswEEP vortex. The fuselage wake is still present and can be seen in the upper left hand corner of Figure 8a.

The hot wire results show a vortex slightly to the right of the upswEEP vortex; this is most likely the empennage induced vortex. However, the main differences between Figures 7 and 8 is namely in the computational result to be unable to determine the

position of the induced vortex. The flow at this location is dominated by these two flow features. The hooked shaped flow structure is again present in both figures. Due to the grid being too coarse it may not be able to determine the characteristics within the hooked shape/ induced vortex region and what is being presented is the tail region of the vortices.



The CFD results have compared reasonably well with those obtained from hot wire. However, in order to determine more of the flow field and its characteristics a more refined grid is called for. The main problems with this work is the relatively small scale of the model, which makes hot wire very difficult near the surface of the model. However, the CFD results presented in this paper agree well with the hot wire near the fuselage. However, away from the fuselage the agreement between hot wire and CFD diminishes, with the present grid.

**Figure 8a and b, ENSICA and CFD results respectively
(For x = +60 mm)**

This can be clarified to some extent when comparing results obtained well away from the model and measured downstream. Where the probe is free to move about without the risk of damage to it or to the model, the probe is able to conduct a detailed study of the flow-field.

Although the computational and experimental work has helped in the understanding of the flow-field around the C-130, due to the small size of the model it was difficult to obtain measurements close to the model. In order to address this problem a second generation wind tunnel model has been developed in order to fully explore the aft flow field of the C130. Due to the new models physical size it is possible to conduct a more extensive survey. The new model is to be used for phase 2 of this project, and is to be used for both clean and tail down investigations. The second generation model is a simplified C130, and consists of a fuselage and rear empennage only. The model is shown below (Figure 9) along with an example grid.

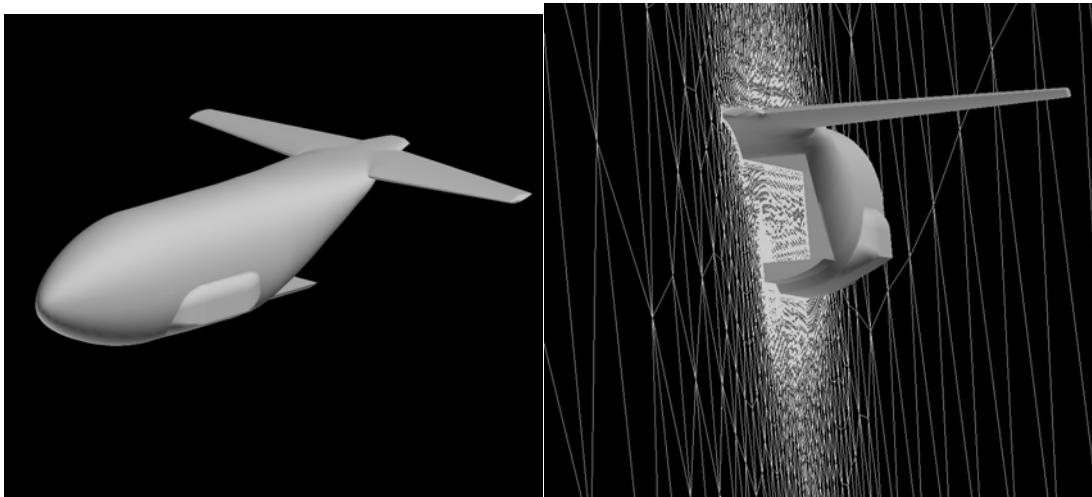


Figure 9, Second C-130 Model showing cargo door and rear cavity. The simplified fuselage is shown to good extent

VI. CONCLUSION

The results have shown a complex flow-field is generated around the rear fuselage of the C130. The experimental hotwire results and the CFD results compare well qualitatively. The hotwire results were limited by the small size of the 1/48th scale wind tunnel model in relationship to the hotwire probe. The CFD data was limited by the grid and needs refinement to accurately capture the vortical flow-field. Due to the findings from the ENSICA experimental and USAFA CFD investigations a second phase of the program has been created to obtain a more detailed understanding of the flow-field. This second phase will be comprised of a much larger simplified version of the C-130 without wings and a more detailed set of CFD simulations.

ACKNOWLEDGEMENTS

The authors gratefully acknowledge the support and CPU hours at the Maui HPCC computing center and Richard Charles U.S Army (NATICK Solider Center) for his funding and support.

REFERENCES

- ¹ Johnson, W., Trickey, C., Forsythe, J., Albertson, J., and Leigh, E., "Experimental and Computational Investigation of the Flow behind a C-130 with Tailgate down," AIAA 2002-0713, January 2002
- ² Galloway, J. D., and McClurg, J. P., "C-130 Firefighting Nozzle Investigation," Department of Aeronautics AE471 Report, USAFA, 1999
- ³ Spalart, P. R., Jou W-H., Strelets M., and Allmaras, S. R., "Comments on the Feasibility of LES for Wings, and on a Hybrid RANS/LES Approach," *Advances in DNS/LES, 1st AFOSR Int. Conf. on DNS/LES*, Aug. 4-8, 1997, Greyden Press, Columbus Oh.
- ⁴ Forsythe, J.R., Hoffmann, K.A., Dieteker, F.F., "Detached-Eddy Simulation of a Supersonic Axisymmetric Base Flow with an Unstructured Flow Solver," AIAA Paper 2000-2410, June 2000.
- ⁵ Pan, J., and Loth, E., "Detached Eddy Simulations for Airfoil with Ice Shapes", AIAA Paper 2004-564, January, 2004
- ⁶ Morton, S.A., Forsythe, J.R., Squires, K.D., and Wurtzler, K.E., "Assessment of Unstructured Grids for Detached-Eddy Simulation of High Reynolds Number Separated Flows," 8th ISGG Conference, Honolulu, June 2002.
- ⁷ Morton, S.A., Forsythe, J.R., Mitchell, A.M., and Hajek, D., "DES and RANS Simulations of Delta Wing Vortical Flows," AIAA 2002-0587, January 2002
- ⁸ Forsythe, J.R., Squires, K.D., Wurtzler, K.E., and Spalart, P.R., "Detached Eddy Simulation of Fighter Aircraft at High Alpha," *AIAA Journal of Aircraft*, Vol. 41, No. 2, 2004, pp. 193-200.
- ⁹ Morton, S., Steenman, M., Cummings, R., and Forsythe, J., "DES Grid Resolution Issues for Vortical Flows on a Delta Wing and an F/A-18C," AIAA 2003-1103, Jan., 2003.
- ¹⁰ Forsythe, J.R., Woodson, S.H., "Unsteady CFD Calculations of Abrupt Wing Stall Using Detached-Eddy Simulation", AIAA 2003-0594, January, 2003.
- ¹¹ Spalart, P., "Young-Person's Guide to Detached-Eddy Simulation Grids," NASA CR 2001-211032
- ¹² Gridgen Version 15.05, Pointwise, www.pointwise.com